J. Trop. Resour. Sustain. Sci. 11 (2023): 29-36
https://doi.org/10.47253/jtrss.v11i1.1093

Journal of Tropical Resources and Sustainable Science

journal homepage: jtrss.org

The effects of magnetic and radiometric responses on hydrothermal zones and its implication in minerals characterization over part of Nasarawa, North Central Nigeria

Abdulsalam Nasir Naeem[1], John Florence Oluwabukola[1], Ologe Oluwatoyin[2, *]

[1]Department of Physics, Faculty of Science, University of Abuja, Abuja, Nigeria
[2]Department of Applied Geophysics, Faculty of Science, Federal University Birnin Kebbi, Nigeria

Received 26 October 2022
Accepted 29 January 2023
Online 30 June 2023

Keywords:
minerals, hydrothermal zones, basement and sedimentary outcrops, Centre for Exploration Targeting (CET), first vertical derivatives(FVD), second vertical derivatives (SVD), total count

⊠*Corresponding author:
Dr. Ologe Oluwatoyin
Department of Applied Geophysics, Faculty of Science, Federal University Birnin Kebbi, PMB 1157, Kebbi State, Nigeria.
Email: oluwatoyin.ologe@fubk.edu.ng

Abstract

Airborne magnetic and radiometric data set over part of Nasarawa, North central Nigeria have been enhanced and interpreted qualitatively. Attributes maps (first and second vertical derivative; and analytic signal maps) from the total magnetic intensity map (TMI) were used to delineate near-surface structures hosting sedimentary rocks forming minerals and differentiate regions based on amplitude responses. The structure trends NE-SW, NW-SE, E-W and N-S directions and the area is predominantly underlain by basement and sedimentary outcrops in the northeastern/western, central portion and southern parts respectively. The total cout map showed the low, moderate and high levels ranged from 6.40 to 14.70 μR/h, 13.31 to 16.66 μR/h and 18.02 to 41.23 μR/h respectively. The Potassium concentration revealed the lowest concentration level (0.02-0.0.16%), moderate level (0.17-0.47%) and highest concentration of (18–27%). The lowest concentration level in the eTh map is related to siltstones and sandstones (Ansh), shale and mudstones (Nsh) and sandstone. The highest level reaches 31.35 ppm in volcanics rocks. The equivalent Uranium concentration map (eU) indicates that the high level of uranium concentration is associated with the black shales, siltstones and sandstones (Ansh) while shale and mudstones (Nsh), sandstones, shale and sandy clay (LaSS), sandstones (Ess), shale and limestones (Esh) and alluvium deposition has the lowest one. The potassium thorium ratio map shows zones characterized by the high K/eTh ratio values that are strong indicators of hydrothermal alteration. From the K/eTh ratio map, it can be observed that the areas affected by the hydrothermal process are featured in pink colour and have a high value of 0.37 in the K/eTh ratio which is an indication of gold mineralisation.

1. INTRODUCTION

Qualitative analysis and interpretation of airborne magnetic and radiometric data have been very useful in identifying anomalous area(s) by delineating geological structures, lithological units, hydrothermal alteration zones and subsurface structures that might host economic and industrial minerals since magnetic minerals are structurally controlled (Abdulsalam et al.,, 2022; Ologe et al.,, 2018). O'leary et al., (1976), Ananaba & Ajakaiye (1987) concluded in their work that deformations are associated with most mineral deposits concentration. Some lineament patterns have been defined to be the most favorable structural conditions in control of various mineral deposits (Megwara & Udensi, 2013; Ananaba 1991, Abdulsalam et al., 2022; Ajakaiye et al., 1986). They often indicate the general geometry of subsurface structures of an area thereby providing a regional structural pattern (Abdulrahaman et al., 2022; Onyewuchi et al., 2012; Ajakaiye et al., 1991). The dependency of Nigeria's economy majorly on oil and gas as the major source of revenue coupled with the dominance of unemployment in the country, demands a need to expand the source of revenue generations in Nigeria. Economic minerals are of importance to the economy of a nation if discovered and harnessed. As this will create a productive environment for business opportunities, boost the nation's economy and provide raw materials for industrial uses which might in turn reduce the level of unemployment thereby eradicating poverty in Nigeria (Adewumi & Salako, 2018). It is therefore important to carry out research like this using high resolution airborne magnetic and radiometric data set of part of Nasarawa State which is endowed with mineral resources. This study is therefore aimed at integrating magnetic and radiometric to delineate mineral potential zone in parts of Nasarawa State.

1.1. Location of the study area

The study location is part of Nasarawa State in North Central Nigeria which is bounded by longitude 8.0oE – 9.0oE and latitude 8.0oN – 9.0oN with an estimated total area of 12,100 km2. The State is accessible by road through Kaduna–Plateau State, Taraba–Benue States and Kogi State – Abuja roads (Figure 1).

eISSN Number: 2462-2389

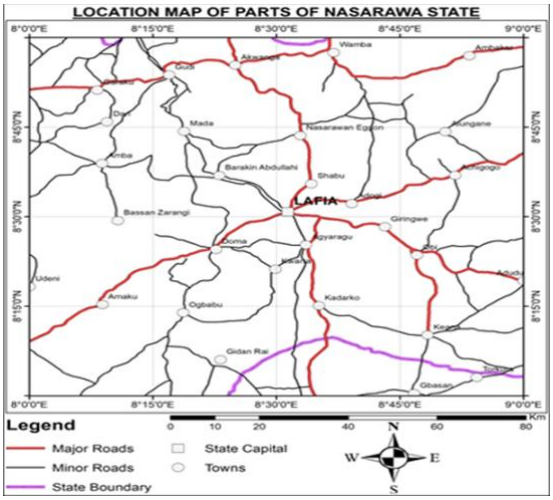

Figure 1: Location map of the study area

1.2. Geology of the study area

The study area is partly located within the middle Benue Trough and partly underlain by the crystalline rocks of the Nigerian Basement Complex. (Figure 2). The Benue Trough is a rift basin in Central West Africa that extends NNE–SSW for about 800 km in length and 150 km in width with 6000 M of Cretaceous to Tertiary Sediment of which those pre-dating the mid-Santonian are compressionally deformed (Benkhelil et al.,, 1988). The Older Granite occupy the areas of Karu, Gurku, Panda, Gitata to the northwest, Keffi, GarakuAkwanga and Nasarawa Eggon to the north-central and Wamba, and environs to the northeast (Anudu et al., 2012, Obaje et al., 2004) while sedimentary rocks cover the southern parts of Nasarawa State. The rocks in Nasarawa State (Figure 2) host Gold in Wamba; Baryte at Azara, Wuse and Aloshi (Anudu et al., 2012); Coals (of the highest rank in Nigeria) at Obi, Jangerigeri, Jangwa and Shankodi; Tantalite at Afu, UdegeBeki, and Wamba; Gemstone in Keffi; Nasarawa Eggon and Kokona; Salt deposits in Ribi, Keana and Awe; Limestone deposits are present in Adudu, and Jangwa; at Keffi, Akwanga, Nasarawa Eggon, TuduUku, etc.

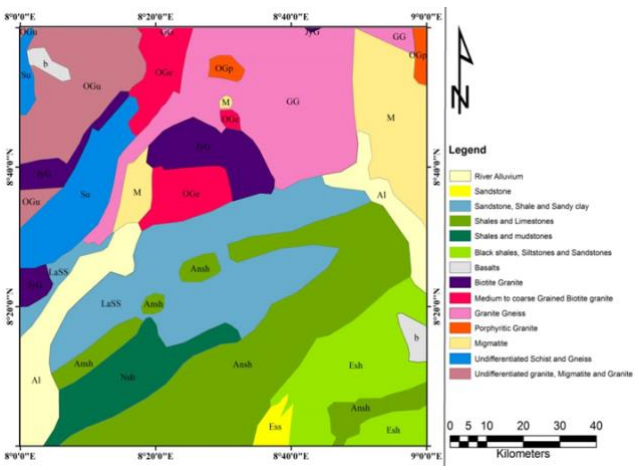

Figure 2: Geological map of the study area

2. MATERIALS AND METHODS

The study area is covered by four aeromagnetic and aeroradiometric data sheets in 1/2º by 1/2º procured from the Nigerian Geological Survey Agency (NGSA). The sheets are 209 (Akwanga), 210 (Wamba), 230 (Doma) and 231 (Lafia). The sheets were assembled and knitted together to generate the composite maps of the study area using Oasis montaj software.

2.1. Data analysis

The early stages of magnetic data analysis generally involve the application of mathematical filters to observed data with the aim of enhancing anomalies of interest and/or gaining some preliminary information on source location or magnetization

2.2.1. Vertical derivative

A vertical derivative tends to sharpen the edges of anomalies and enhance shallow features. The Vertical derivative map is much more responsive to local influence than to bread or regional effect. Therefore, a vertical derivative tends to give a sharper picture than the map of the total field.

$$L(r) = r^n \quad (1)$$

Where n is the order of differentiation, r is the wave number in radians/ground unit. Ground unit means survey used in the grid, examples are meters and feet.

2.2.2. Analytical signal

The 3D analytic signal A of a potential field anomaly can be defined as (Nabighian, 1984).

$$A(x,y,z) = \left[\frac{\partial M}{\partial x}\right]\hat{x} + \left[\frac{\partial M}{\partial y}\right]\hat{y} - j\left[\frac{\partial M}{\partial z}\right]\hat{z} \quad (2)$$

Where M = magnetic field, this concept was introduced by Nabighian in 1974.

2.2.3. Centre for exploration targeting (CET)

Starting with standard deviation**,** which provides an estimate of the local variation in the data. At each location in the grid, it calculates the standard deviation (σ) of the data values within the local neighbourhood, N cells with mean value μ and cell values x_i is given by:

$$\sigma = \sqrt{\frac{1}{N}\sum_{i=1}^{N}(x_{i-}\mu)^2} \quad (3)$$

The output can be interpreted as the one with very little variation and high variation when the values approach zero and large values respectively (Kovesi, 1991). Centre for exploration targeting was carried out to recognise linear structures contained within the aeromagnetic data through a repeated map by product forms that include standard deviation which determines variations in magnetic response (Abdulsalam et al., 2022), and the

eISSN Number: 2462-2389

continues lines can be separated with phase symmetry. Afterwards, the resulting lineaments were enhanced by suppressing noise and background signals using amplitude thresholding (Figure 7).

2.2.4. Source Parameter Imaging (SPI)

The SPI of aeromagnetic fields over the area differentiated and characterised regions of sedimentary thickening from shallow basemenst and also determine the depths to the magnetic sources. In this case, mineral deposits including hydrocarbon presence can easily be suggested from the results.

SPI assumes a step-type source model.

$$Depth = {}^{1}\!/\!_{K_{max}} \quad (4)$$

Where K_{max} is the peak value of the local wavenumber K over the step source.

$$\text{Tilt derivative A} = \tan^{-1}\left(\frac{\frac{dT}{dz}}{\sqrt{\left(\frac{dT}{dx}\right)^2+\left(\frac{dT}{dy}\right)^2}}\right) \quad (5)$$

T = the total magnetic field anomaly grid.

2.2. Analysis of radiometric data

To display the three primary variables measured, three maps were produced percentage potassium (%K), equivalent Uranium (eU), and equivalent Thorium (eTh) (Ostrovskiy 1975). Other derived products were also useful, including a K/eTh map, ternary K-eU-eTh radioelement maps in Red-Green-Blue and composite radioelement maps. The resulting images comprise colors generated from the relative intensities of the three components and represent subtle variations in the ratios of the three bands. A histogram equalization to give the best color variation was used to enhance the contrast of the individual histograms of K, Th and U before combining them with the composite image. Different rock types are often characterized by specific radiometric elements ratios, therefore, the ternary maps of these ratios are useful geological and mineral exploration tools for discriminating lithologies. The four composite color images (maps) that were prepared from their respective ratios are as follows:

I K, eU and eTh (three radioelements composite image map)
II K, K/eU and K/eTh (potassium composite image map)
III eU, eU/eTh and eU/K (equivalent uranium composite image map)
IV eTh, eTh/eU and eTh/K (equivalent thorium composite image map

Three radioelements composite image map is produced by using different ink colors to represent the K (in per cent), eU (in ppm) and eTh (in ppm) concentrations. This distinct relationship between color hue and ternary ratio allows the map to display surface radioelement distribution (Mohamed, 2013).

3. RESULTS AND DISCUSSION

The airborne magnetic and radiometric data set over a part of Nasarawa, North central Nigeria has been enhanced, analysed and interpreted qualitatively and quantitatively by applying a number of selected digital filters to delineate subsurface structures so as to identify mineral potential zones in the study area. Figure 3 (Total magnetic intensity map) enabled the identification of structures, trends and domains of varying intensities, signatures and frequencies. The high frequencies at the northern part of the study area suggest that this portion of the study area is dominated by crystalline rocks while the southern portion is made up of sedimentary rocks. The TMI was produced after removal of IGRF of 33,000 nT in colour aggregate, with pink to red colour depicting high magnetic anomalies while green to blue depicts low magnetic anomalies ranging from –41.4 nT to 113.9 nT (Figure 3) with high magnetic signature trending NE-SW. While the low magnetic signature which is of sediment deposition also occupies the central part down to the southern part of the study area, an area which corresponds to part of Nasarawa Eggon, Doma, Lafia and its environs. The greenish part of the study area indicates alluvium deposition (Obaje et al., 2007), which is more pronounced in the southern part and corresponds to part of Lafia agreeing with the geological map of the study area (Figure 2). The first vertical derivative (Figure 4) filter aided in revealing near surface magnetic lineaments that trends NE-SW. The map is made up of the basement and sedimentary regions with a clear boundary separating the basement and the sedimentary portions of the study area at Nasarawa eggon; the basement occupies the northern portion while the sedimentary takes the southern portion of the area of study. One of the significant applications of the first vertical derivative is identifying magnetic lineament and determining the border between lithological units more precisely trending in the northeast-southwest direction within the study area. Since magnetic minerals are structurally controlled, the structures found in the study area might host minerals such as gold at Wamba; Tin, Columbite and Tantalite at Akwanga and Granitic rocks at Nasarawa Eggonin the study area. The second vertical derivative map (Figure 5) emphasizes the near surface features such as late-stage dykes, veins, contacts and cultural sources that have been removed from the regional data (Ologe et al, 2018).

It also reveals the presence of faults and shear zones. The trend of structures identified on the first vertical derivative map agrees with the trend of the structures (lineaments) delineated on the second vertical derivative map (Ologe et al., 2018, Abdulrahman et al., 2022).

eISSN Number: 2462-2389

J. Trop. Resour. Sustain. Sci. 11 (2023): 29-36
https://doi.org/10.47253/jtrss.v11i1.1093

Journal of Tropical Resources and Sustainable Science

journal homepage: jtrss.org

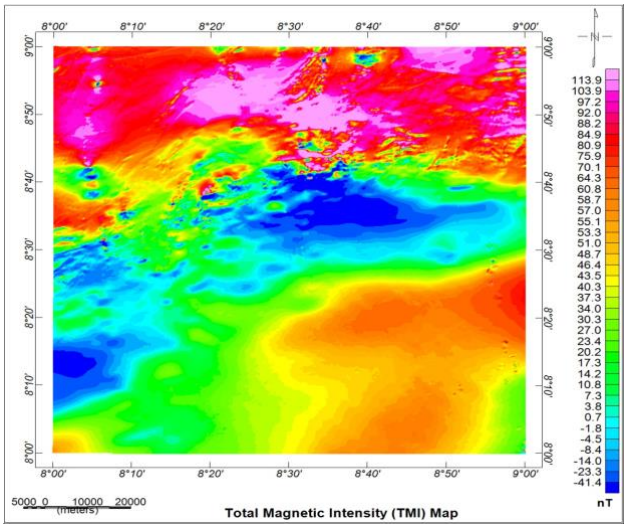

Figure 3: Total Magnetic Intensity of the Study Area. (After removal of IGRF, a sum of 33,000 nT removed for purpose of handling must be added to get the actual value at any point)

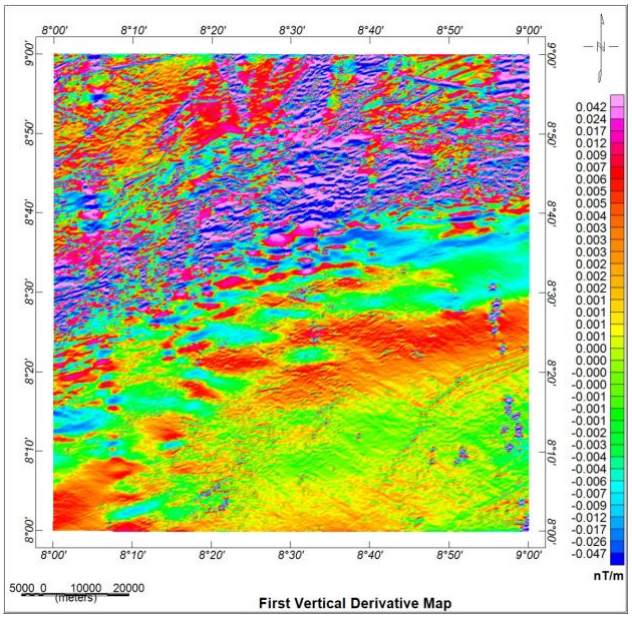

Figure 4: First Vertical Derivative Map of the study Area

The analytical signal map (Figure 6) exposes the variations in amplitudes of the magnetic anomalies which help in delineating the study area into regions of an outcrop, intermediate structures and basement under the influence of thick sedimentation. Two major regions can clearly be observed; regions whose amplitude responses are high ranging from 0.024 m to 0.98 m which are predominantly basement outcrops with varying degrees of deformations at the northeastern, central portion and the northwestern part of the study area; and regions whose amplitude are low ranging from 0.001 to 0.006 (Figure 6), which represents regions with relatively good sedimentation at the southern part of the study area (Ologe et al., 2018). It is worth mentioning that the lineaments exhibited by the vectorisation map (Figure 7) reveal the basement rocks that occupy the northern part of the area are highly deformed as compared with the southern part covered by cretaceous sedimentation (Anudu et al., 2012). Figure 7 shows prominent lineaments trending in the direction NE-SW, NW-SE, NNE-SSW and NNW- with few ones trending in the N-S direction, this was corroborated in the work of Anudu et al., 2011 and Anudu et al., 2012. A large number of faults and shear zone have been identified using several filtered techniques mostly the first vertical derivative, analytic signal and vectorization. To complement the geologic contact map (Figure 8), which is based on the automated lineament detection output and the traced ones from the first vertical derivative and analytic signal. This displayed the relationship between the expected complexity structural zones and known gold mineralization which was indicated in the geologic map of the study area.

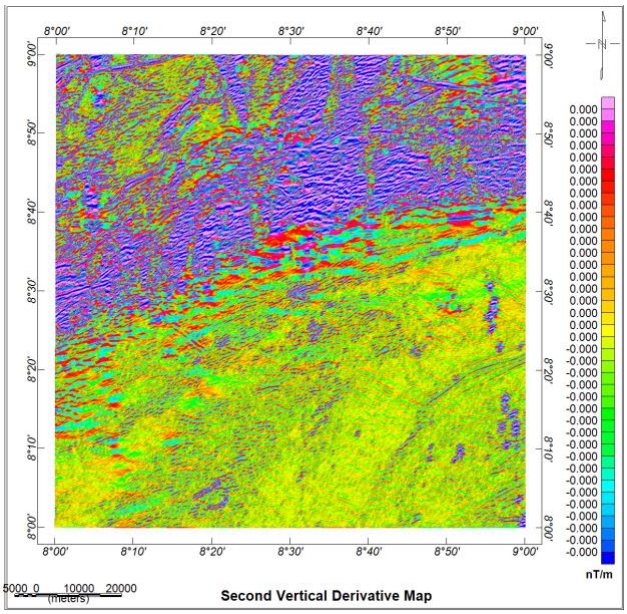

Figure 5: Second vertical derivative map of the study area

eISSN Number: 2462-2389

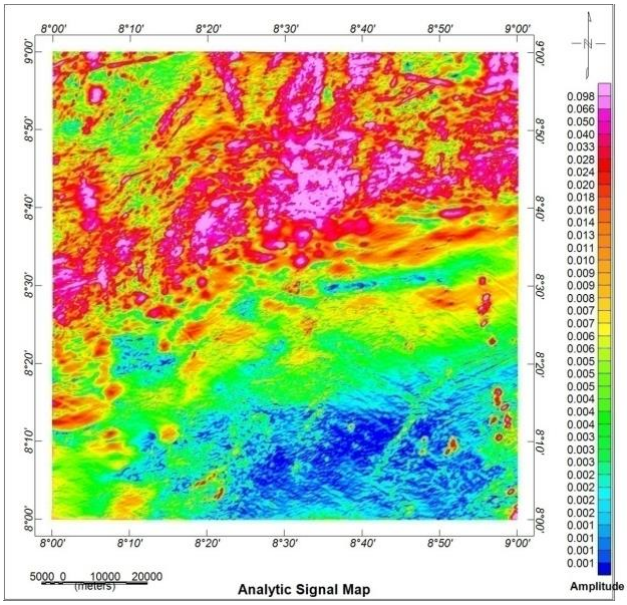

Figure 6: Analytic signal map of the study area

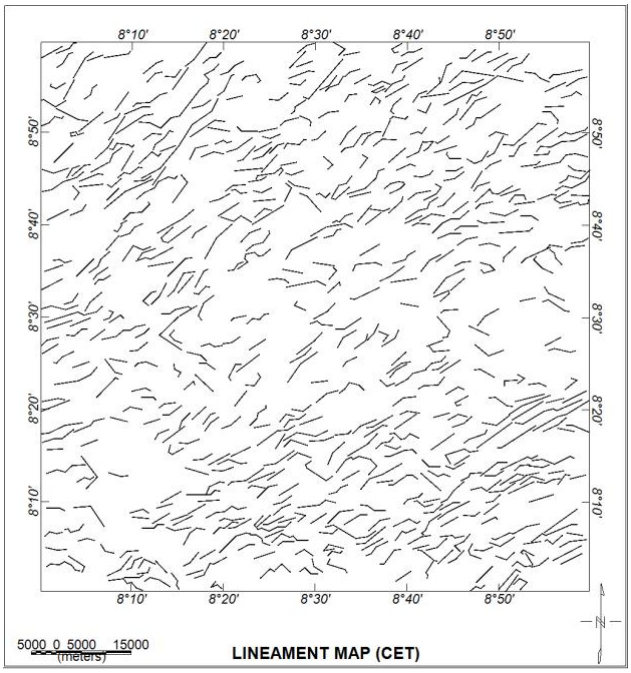

Figure 7: Lineament map (CET) of the study area

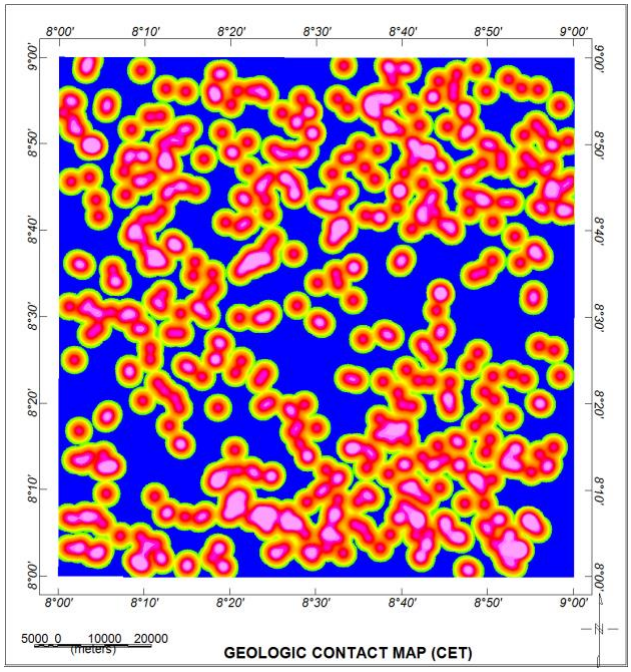

Figure 8: Geological contact map of the study area

3.1 Results of Total Count (TC) of radioactive elements

The lowest concentration level measured in count per hour ranges from (6.40 to 14.70 μR/h) as shown in the total count map (Figure 9). This is associated with Siltstones and sandstones (Ansh), Shale and Mudstones (Nsh), Sandstones, Shale and Sandy clay (LaSS), Sandstones (Ess), Shale and Limestones (Esh). The moderate concentration level ranging from (13.31 to 16.66 μR/h) is observed at the south-eastern part of the study area and is related to Lafia formation. The high level concentration that ranges from (18.02 to 41.23 μR/h) is associated with Biotite Granite, Granite Gneiss, Porphyritic Granite, Migmatite, Schist and Gneiss (Figure 9). The Potassium (K) Concentration map (Figure 10) shows that Siltstones and sandstones (Ansh), Shale and Mudstones (Nsh), Sandstones, Shale and Sandy clay (LaSS), Sandstones (Ess), Shale and Limestones (Esh) have lowest concentration level (0.02-0.0.16%). While, the metasediments (ms), Lafia formation have the moderately level (0.17-0.47%); Biotite Granite, Granite Gneiss, Porphyritic Granite, Migmatite, Schist and Gneiss have the highest concentration of (18–27%). The lowest concentration level in the eTh map (Figure 11) is related to Siltstones and sandstones (Ansh), Shale and Mudstones (Nsh) and Sandstone. The highest level reaches by Biotite Granite, Granite Gneiss, Porphyritic Granite, Migmatite, Schist and Gneiss is 31.35 ppm.

eISSN Number: 2462-2389

The

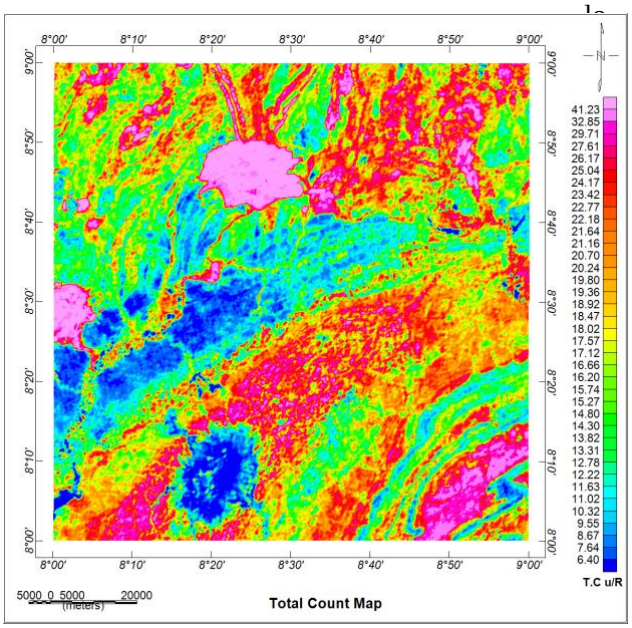

Figure 9: Total count map of the study area

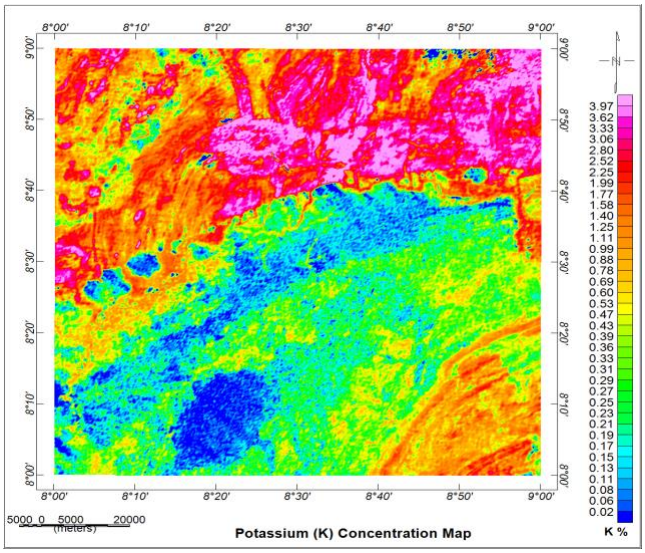

Figure 10: Potassium (K) concentration map of the study area

The equivalent Uranium concentration map (eU) (Figure 12) indicates that the high level of uranium concentration is associated with the Siltstones and sandstones (Ansh), Shale and Mudstones (Nsh), Sandstones, Shale and Sandy clay (LaSS), Sandstones (Ess), Shale and Limestones (Esh) and Alluvium deposition have the lowest one. It was glaring that there is a near agreement between the indicated levels of radioactivity and the corresponding rock types. The major linear trend, which could be interpreted from the elongation of the radiometric anomalies is the NE-SW trend. Consequently, the NE-SW trend seems to be the most delineated trend from both aeromagnetic and aeroradiometric interpretation (Andrson & Nash 1997), and that confirms the effective role of this trend. Some other trends (NW-SE, E-W and N-S) could be traced from other elongated bodies of the radiometric anomalies.

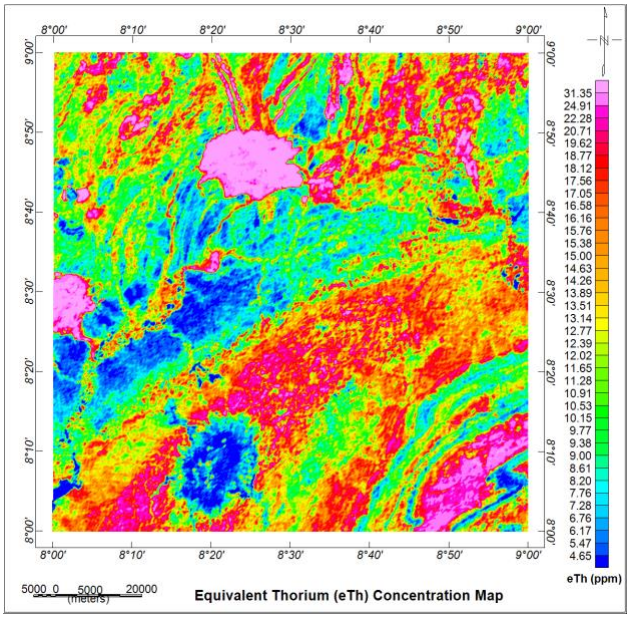

Figure 11: Equivalent Thorium (eTh) concentration map of the study area

As potassium is more transportable than thorium, K/eTh ratio anomalies can be distinguished to areas of hydrothermal alteration which are characterized by K enrichment. However, it was made known that the ratio between potassium and thorium is constant in most rocks varying from 0.17 to 0.2 (K/Th in %/ppm, Darnley et al., 1989). Rocks with K/eTh ratios remarkably outside of this range have been named potassium or thorium specialized (Elkhateeb & Abdellatif 2018) with hydrothermal alteration zones showing high K/eTh ratio values. From the K/eTh ratio map (Figure 13), it was observed that the areas affected by the hydrothermal process are featured in pink colour and have a high value of about 0.37 of the K/eTh ratio. These areas are associated with Biotite Granite, Granite Gneiss, Porphyritic Granite, Migmatite, Schist and Gneiss in the northeastern and northwestern part of the study area. Also, the map clearly showed that the interpreted alteration zones were following the NE-SW trend which was inferred as the major trend in the area of investigation.

The ternary map (Figure 14) of the study area was produced by modulating the three colours red, green and blue for the intensities of Potassium, thorium and uranium respectively. The radiometric response in the ternary map to some extent corresponds with the surface rock units of the study area and shows a close spatial correlation with the geologic map (Figure 2). A close look at this map shows that high concentrations of K, eTh and eU radioactive elements are displayed in red colour and related to Biotite Granite (JyG), Metamorphic rocks (gnl), Medium to coarse Grained Biotite granite (OGe) and Granite Geniss (vf). They are usually categorized by their strong radiometric signature and can be easily distinguished from low radioactive rocks. A low concentration of K, eTh, and eU radioactive elements is signified by dark colour corresponding with Porphyritic Granite (OGp), Migmatite (m), and Talc Carbonate rocks

eISSN Number: 2462-2389

(sp). The red colour represents high potassium content but low thorium and uranium and coincides with undifferentiated Schist and Gneiss (Su) and undifferentiated granite, Migmatite and Granite (OGu). Also, the green color corresponds to regions of high thorium with low potassium and uranium associated with Sandstone, Shale and Sandy clay (LaSS). And the blue colour corresponds to regions of high uranium with low thorium and potassium associated with Shale and Limestones (Ansh), Shale and Mudstones (Nsh), Black shales, Siltstones and sandstones (Esh).

A careful inspection of this map and its rapprochement with the geological map of the study area (Figure 2) highlights some conspicuous features making those contacts (basement and sedimentary) more obvious. Most of the traced rock units of the basement complex such as Biotite Granite (JyG), Metamorphic rocks (gnl), Medium to coarse Grained Biotite granite (OGe) and Granite Geniss (vf) are in close agreement with the rock units presented in the geological map of the study area.

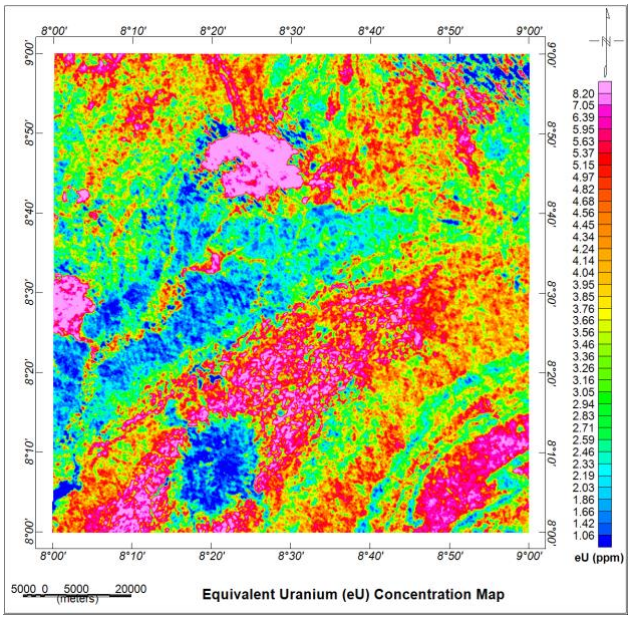

Figure 12: Equivalent Uranium (eU) concentration map of the study area

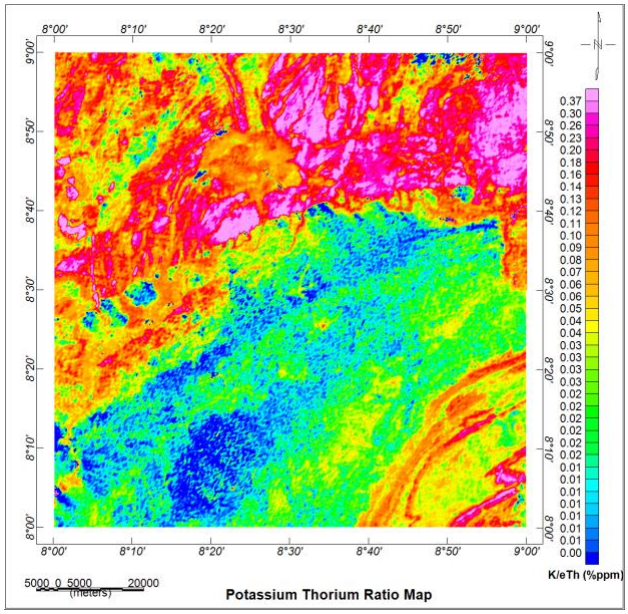

Figure 13: Potassium thorium ratio map of the study area

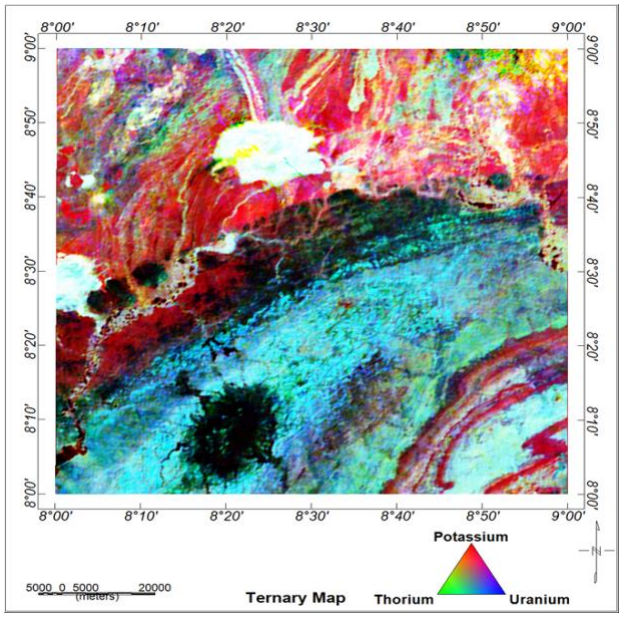

Figure 14: Ternary map of the study area

3.2. Data integration

The results of the analysis of aeromagnetic and aeroradiometric data sets showed that the northern part of the study area is extremely faulted compared to the southern part. The predominant tectonic trends are NW, NNW, NNE, NE-SW, NW-SW NE, and E-W. The NE-SW was the most developed one among these trends and represents the preferred orientation of Gold deposits at Wamba. Also, a number of hydrothermally altered zones are mapped from the K/eTh ratio map (Figure 13). Since these zones have one or more structure associations, they serve as channel corridors for migrating hydrothermal fluids that contemporaneously react with rock formation which got altered subsequently. The alteration zones are marked by low magnetic intensity and high potassium content that lie within or close to a structure that has a NE trend delineated before. The coincidence areas of these

eISSN Number: 2462-2389

alteration zones and high complexity lineaments indicated a high possibility for the occurrence of gold mineralization in other similar locations. The aeroradiometric maps assisted in correlating the distribution of the radioactivity elements with the rock units, mapping of lithology and hydrothermal alteration zon es. A strong indicator for hydrothermal alteration zones are as a result of the K/eTh ratio map high valued.

4. CONCLUSION

The analysis and interpretation of high resolution of airborne magnetic and the radiometric data set of part of Nasarawa State have been carried out. The near surface structures (lineaments) which might host potential minerals in the study area and the hydrothermal alteration zones have been delineated. The predominant tectonic trends are NW,NNW, NE-SW,NW-SW,NE,E-W and N-S.

The NE-SW was the most developed one among these trends and represents the preferred orientation of Gold deposits at Wamba. The coincidence areas of these alteration zones and high complexity lineaments indicated a high possibility for the occurrence of gold mineralization in other similar locations. Based on the lineaments delineated and the hydrothermal alterations, it is recommended that the study area should be subjected to further investigation using active geophysical methods to ascertain the occurrence of minerals in the basement portion of the study area that could contribute to the growth of the Nigerian economy.

ACKNOWLEDGEMENT

Special thanks to the Department of Physics, University of Abuja for providing the enabling environment to carry out the interpretation and analysis of this research. The management of Nigeria Geological Survey Agency (NGSA) is well appreciated for the release of the airborne magnetic and radiometric dataset.

REFERENCES

Abdulsalam N. N., Ogoh E. K. & Ologe O., 2022. Evaluation of Structural Framework and Depth Estimates Using High Resolution Airborne Magnetic Data over Some Parts of Middle Benue Trough, Nigeria. International Journal of Geosciences , 13, 557-575. https://doi.org/10.4236/ijg.2022.137030.

Augie A.I., Salako K.A., Rafiu A.A. & Jimoh M.O., 2022. Geophysical assessment for gold mineralization potential over the southern part of Kebbi State using aeromagnetic data.Geology,Geophysics and Environment, 48, 2, 177–193. https://doi.org/10.7494/geol.2022.48.2.177.

Adewumi T., &Salako K.A. 2018. Delineation of mineral potential zone using high resolution aeromagnetic data over part of Nasarawa State, North Central, Nigeria. Egyptian journal of petroleum, 27, 4, 759-767.

Ajakaiye D.E., Hall D.H., Ashiekaa J.A. & Udensi, E.E. 1991. Magnetic anomalies in the Nigerian continental mass based on aeromagnetic surveys. Tectonophysics, 192, 211-230

Ajakaiye D.E., Hall D.H., Miller T.W., Verhergen P.J.T., Awad M.B. & Ojo S.B. 1986. Aeromagnetic anomalies and tectonic trends in and around the Benue Trough, Nigeria. Nature, 319, 582-584.

Ananaba S.E. & Ajakaiye D.E. 1987. Evidence of tectonic control of mineralization in Nigeria from lineament density analysis A Landsat-study. International Journal of Remote Sensing, 8,10, 1445-1453.

Ananaba S.E. 1991. Dam sites and crustal magalineaments in Nigeria.ITC Journal, 1, 26-29

Andrson H. & Nash C. 1997. Integrated lithostructural mapping of the Rossing area, Namibia, using high-resolution aeromagnetic, aeroradiometric, Landsat data and aerial photographs. Explor.Geophys. 28, 185–191.

Anudu G.K., Onuba L.N., Onwuemesi A.G. & Ikpokonte A.E. 2012. Analysis of aeromagnetic data over Wamba and its adjoining areas in North-central Nigeria. Earth Science and Resistivity Journal, 16, 1, 25-33

Anudu G.K., Essien B.I., Onuba L.N. & Ikpokonte A.E. 2011. Linearment analysis and interpretation for assesment of groundwater potential of Wamba and adjoining areas. Journal of Applied Technology in Environmental Sanitation, 1, 185-198

Benkhelil J., Guiraud M., Ponsard J.F., Saugy L. 1988. The Bornu–Benue Trough, the Niger Delta and its offshore: Tectono-sedimentary reconstruction during the Cretaceous and Tertiary from geophysical data and geology. Geology of Nigeria.2nd ed. Rock view, Jos

Implications–Examples from the Hokusatsu Region of SW Kyushu, Japan–. Resource Geology, 48(2), 75-86.

Darnley A.G., Ford K.L. & Garland G.D. 1989. Regional airborne gamma-ray surveys: a review, in: Proceedings of Exploration ' 87: Third Decennial International Conference on Geophysical and Geochemical Exploration for Minerals and Groundwater. Geological Survey of Canada, special. 3, 960.

Elkhateeb S.O. & Abdellatif M.A.G. 2018. Delineation potential gold mineralization zones in a part of Central Eastern Desert, Egypt using Airborne Magnetic and Radiometric data. NRIAG Journal of Astronomy and Geophysics, 7, 2, 361-376.

Kovesi P. 1991. A dimensionless measure of edge significance.In The Australian Pattern Recognition Society, Conference on Digital Image Computing: Techniques and Applications. 281-288

Megwara J.U. & Udensi E.E. 2013. Lineaments study using aeromagnetic data over parts of southern Bida basin, Nigeria and the surrounding basement rocks. International Journal of Basic and Applied Sciences, 2, 1, 115.

Mohamed A.S., Youssef M.A & Shadia S.T. 2013. Utilization of airborne gamma ray spectrometric data for geological mapping, radioactive mineral exploration and environmental monitoring of southeastern Aswan city, South Eastern Desert, Egypt. Geophysical Journal International, 195,3, 1689-1700

Nabighian M.N. 1974. Additional comments on the analytic signal of two-dimensional magnetic bodies with polygonal cross-section. Geophysics, 39,1, 85-92.

Nabighian M.N. 1984. Toward a three-dimensional automatic interpretation of potential field data via generalized Hilbert transforms: fundamental relations. Geophysics. 49, 6, 780–786.

Obaje N.G., Jauro A., Agho M.O., Abubakar M.B., Tukur A. 2007. Organic geochemistry of Cretaceous Lamza and Chikila coals, upper Benue trough, Nigeria, Fuel. 86, 4, 520–532.

Obaje N.G., Wehner H., Abubakar M.B., Isah M.T., Nasara I. 2004. Gongola Basin (Upper Benue Trough, Nigeria): source-rock evaluation, J. Pet. Geol. 27,2, 191–206.

O'leary D.W., Friedman J.D. & Pohn H.A. 1976. Lineament, linear, lineation: some proposed new standards for old terms. Geological Society of America Bulletin. 87, 10, 1463-1469.

Ologe O., Mallam A. & Abdulsalam N.N. 2018. Application of Aeromagnetic Data in Delineating Structural Patterns in Kebbi State, Northwestern, Nigeria. Minna Journal of Geosciences, 2, 2, 82-94

Onyewuchi R.A., Opara A.I & Oko F.U. 2012. Interpretation of Structural and Geomorphic Features from aeromagnetic and Landsat Data: Case Study of Nkalagu Area, Southeastern

eISSN Number: 2462-2389

Nigeria. International Journal of Science and Technology. 2, 3, 340-350

Ostrovskiy E.A. 1975. Antagonism of radioactive elements in wallrock alteration fields and its use in aerogamma spectrometric prospecting. Int. Geol. Rev. 17, 4, 461–468

eISSN Number: 2462-2389